Glucocorticoids ameliorate cardiorenal syndrome through the NPR1/SGK1 pathway in natriuretic peptide receptor A-heterozygous mice

YAO-MENG HUANG[1], TONG-XIN LI[1], SHU-YU LI[1,2], XIAO-RAN ZHU[1,3], YING LI[1], DANG-YANG LIU[1], WEI-MIN LI[1], LIN-QUAN YANG[3], KUN-SHEN LIU[1] and CHAO LIU[1]

[1]The First Cardiology Division, The First Hospital of Hebei Medical University, Shijiazhuang, Hebei 050030; [2]Department of Cardiology, Affiliated Hospital of North China University of Science and Technology, Tangshan, Hebei 063210; [3]Department of Pharmacy, Hebei General Hospital, Shijiazhuang, Hebei 050057, P.R. China

Received February 11, 2022; Accepted April 28, 2023

DOI: 10.3892/etm.2023.12073

Abstract. Natriuretic peptides, which are produced by the heart, bind to natriuretic peptide receptor A (NPR1 encoded by natriuretic peptide receptor 1 gene) and cause vasodilation and natriuresis. Thus, they serve an important role in regulating blood pressure. In the present study, microinjection of CRISPR associated protein 9/single guide RNA into fertilized C57BL/6N mouse eggs was performed to generate filial generation zero (F0) Npr1 knockout homozygous mice ($Npr1^{-/-}$). F0 mice mated with wild-type (WT) mice to obtain F1 Npr1 knockout heterozygous mice with stable heredity ($Npr1^{+/-}$). F1 self-hybridization was used to expand the population of heterozygous mice ($Npr1^{+/-}$). The present study performed echocardiography to investigate the impact of NPR1 gene knockdown on cardiac function. Compared with those in the WT group (C57BL/6N male mice), the left ventricular ejection fraction, myocardial contractility and renal sodium and potassium excretion and creatinine-clearance rates were decreased, indicating that Npr1 knockdown induced cardiac and renal dysfunction. In addition, expression of serum glucocorticoid-regulated kinase 1 (SGK1) increased significantly compared with that in WT mice. However, glucocorticoids (dexamethasone) upregulated NPR1 and inhibited SGK1 and alleviated cardiac and renal dysfunction caused by Npr1 gene heterozygosity. SGK1 inhibitor GSK650394 ameliorate cardiorenal syndrome by suppressing SGK1. Briefly, glucocorticoids inhibited SGK1 by upregulating NPR1, thereby ameliorating cardiorenal impairment caused by Npr1 gene heterozygosity. The present findings provided novel insight into the understanding of cardiorenal syndrome and suggested that glucocorticoids targeting the NPR1/SGK1 pathway may be a potential therapeutic target to treat cardiorenal syndrome.

Correspondence to: Professor Chao Liu, The First Cardiology Division, The First Hospital of Hebei Medical University, Hebei Medical University, 89 Donggang Road, Shijiazhuang, Hebei 050030, P.R. China
E-mail: dr.liuchao@gmail.com

Key words: glucocorticoid, cardiorenal syndrome, natriuretic peptide receptor A, serum/glucocorticoid regulated kinase 1

Introduction

Members of the natriuretic peptide (NP) family, such as atrial natriuretic peptide (ANP), brain natriuretic peptide (BNP) and C-type natriuretic peptide (CNP), serve important physiological functions in maintaining cardiovascular homeostasis (1,2). ANP and BNP are primarily synthesized in the heart tissues and circulate in blood, while CNP is mainly produced by vascular endothelial cells and may mediate physiological effects, such as cardiomyocyte contractility, reproduction, cell proliferation (2,3). These peptides exert their effects by binding to NP receptors (NPRs) 1, 2 and 3. NPR1, which binds to ANP and BNP, and NPR-B, which is selective for CNP, (2,3) are composed of an extracellular ligand-binding, a transmembrane, an intracellular kinase homology and a C-terminal guanylate cyclase domain (4). In addition, NP-scavenging receptor (also known as NPR-C) lacks guanylate cyclase activity and mediates NP degradation (5).

NPR1 is expressed in different tissue and cells and mediates a variety of central and peripheral effects of ANP and BNP, which contribute to lowering blood pressure (1,6). NPR1 is a transmembrane receptor coupled with granular guanosine cyclase, which promotes synthesis of the second messenger cyclic guanosine monophosphate (cGMP). cGMP regulates activity of specific effector molecules, including cGMP-dependent protein kinase G, cyclic nucleotide-gated cation channels and phosphodiesterase subtypes, thereby regulating biological processes associated with vascular tension, intestinal secretion, bone growth, arterial blood pressure and volume homeostasis (7-9). The targeted deletion of ANP or NPR1 can lead to severe chronic arterial hypertension (9,10). In addition, NPR1 deletion causes severe damage to the heart and kidney and significantly decreases survival rate in mice (11). However, an animal model of cardiorenal syndrome, specifically in Npr1 heterozygous

mice ($Npr1^{+/-}$ mice), has not yet been established. Although the phenotype of NPR1 knockout mice is known, the implementation of long-term experiments is limited by their short lifespan (11). On this basis, the selection of $Npr1^{+/-}$ mice for the present study not only ensured partial NPR1 deletion but also met the need for long-term experiments (12,13).

Serum glucocorticoid-regulated kinase 1 (SGK1) upregulates expression of the epithelial sodium channel (ENaC), promoting sodium reabsorption and decreasing renal sodium excretion (14,15). The expression of NPR1 is positively regulated by SGK1 and NPR1 participates in renal sodium excretion (16), but whether NPR1 can regulate SGK1 expression, especially in the kidney, remains unclear.

The present study established a $Npr1^{+/-}$ mouse model by deleting exon 1, including the 5'-untranslated region (UTR) of Npr1, and aimed to examine the effects of glucocorticoids, such as dexamethasone, on cardiorenal syndrome caused by Npr1 gene knockdown and the underlying mechanisms.

Materials and methods

Gene targeting. All experiments involving animals were approved by the Ethics Review Committee for Animal Experimentation of the Hebei Medical University (Shijiazhuang, China (approval no. 20210909). Mice with global deletion of NPR1 were constructed by Beijing Biocytogen Co., Ltd. based on transcript-NM_008727.5. The structure of the Npr1 gene was showed in National Center for Biotechnology Information (NCBI) (ncbi.nlm.nih.gov/gene/?term=18160). The protocol used for the gene targeting experiments was as previously published (17). The study design is shown in Fig. 1A. In brief, single guide RNAs (sgRNAs) at the 5'- and 3'- target sites were designed by Wellcome Sanger Institute Genome Editing (2020 version, Wellcome Sanger Institute; Fig. 1B and C). Oligos were synthesized and ligated into the pCS-4G vector using the Gibson method (Fig. 1C) (18). The sequence of recombinant plasmid was verified by checking sequence after transforming the recombinant plasmid into *Escherichia coli* by $CaCl_2$ method (19). sgRNA 1 and 12 were selected to generate a ~4.0-kb chromosomal deletion (exon 1) at the extreme genome editing -WYS-006-A locus in the mouse genome according to CRISPR-associated protein 9 (Cas9)/sgRNA activity based on their activity and specificity (Fig. 1D). Cas9/sgRNA was microinjected into fertilized mouse ova to obtain male heterozygotes, which were mated with C57BL/6N female mice. The inactivated Npr1 gene was transferred to the first filial generation (F1).

CRISPR/Cas9 activity detection. Candidate sgRNA expression plasmid (CAS9P; Sigma-Aldrich) and the plasmid containing the CRISPR/Cas9 target sequence pUCA (Luc)-target reporter gene were transfected into fertilized C57BL/6N mouse ova. Because the Luc gene contained a termination codon and target sequence, the termination codon and target sequence are complementary repeat sequences of Luc at both ends. The termination codon leads to the early termination of Luc translation and expression of non-functional luciferase. The cleavage of the target site by nuclease triggers the DNA repair mechanism based on Single-Strand Annealing (SSA), and the complementary repeat sequence forms a complete luciferase coding sequence through recombination, thus expressing functional luciferase.

Animal preparation and diet. A total of 50 8-week-old male mice (including 17 C57BL/6N wild-type (WT) and 33 $Npr1^{+/-}$ mice) with a mean weight of 20 g were housed in cages at 18-22˚C) and humidity (50-60%) and a 12/12-h light/dark cycle. They were provided with normal mouse diet *ad libitum*. GSK650394 (HY-15192, Sigma-Aldrich), a selective inhibitor of SGK1, was used to inhibit SGK1 activity. Dexamethasone sodium phosphate (cat. no. D424703, Aladdin) was used as a representative glucocorticoid to observe the effects on mouse heart and kidney function.

The mice were assigned to the following groups: i) WT (n=13); ii) $Npr1^{+/-}$ (n=16); iii) WT + DEX (WT mice treated with 1 mg/kg dexamethasone intraperitoneal injection, n=4); iv) DEX + $Npr1^{+/-}$ ($Npr1^{+/-}$ mice treated with 1 mg/kg dexamethasone intraperitoneal injection, n=13) and v) $Npr1^{+/-}$ + GSK650394 ($Npr1^{+/-}$ mice treated with 10 mg/kg/day GSK650394 intraperitoneal injection once daily for 10 days, n=4). Mice were placed in metabolic cages for environmental acclimatization 3 days before the start of the experiments. Urine samples were collected for physiological analysis 12 h after the intraperitoneal injection of dexamethasone. Both dexamethasone and GSK650394 used physiological saline (0.9%) as the carrier and the WT and $Npr1^{+/-}$ groups received physiological saline to reduce inter-group error. In the GSK650394-treated mice group, urine was collected within 12 h of the last injection of GSK650394. All urine was collected for evaluating excretion of urinary sodium, potassium, nitrogen and creatinine through automatic biochemical analyser (cat. no. AU5800, Beckman Coulter). Cardiac function was evaluated using echocardiography. After 12 h glucocorticoid treatment, the mice were sacrificed by cervical dislocation. The heart or kidney tissue was perfused and removed, then fixed overnight in 4% paraformaldehyde. Tissue was dehydrated in a 30% sucrose solution at 4˚C for overnight. Following this, the tissue was embedded in OCT and frozen in liquid nitrogen for later use. The fixed tissue was sectioned (5 μm thickness) at the maximum transverse diameter of the tissue in a -20˚C. Sections were taken for immunofluorescence (IF) and immunohistochemistry (IHC) staining. In addition, left ventricular heart and medullary kidney tissues were excised for western blotting.

Identification of mouse genotype and PCR. The tail tip of each mouse was removed after anesthesia and placed the mouse tip in 0.5 ml centrifuge tube and adding 60 μl of digestive solution A [5 mM NaOH (cat. no. 1310-73-2; Millipore), 0.2 mM EDTA (cat. no. E8030, Solarbio)]. Next, 60 μl solution B (40 mM Tris HCl, pH 5.5, cat. no. T8230; Beijing Solarbio) was added in centrifuge tube and mixed by vortex shaking. The supernatant was used as PCR amplification template following centrifuge the tube at 13,400 x g, 4˚C for 2 min. EGE-WYS-006-A-WT-forward(F),EGE-WYS-006-A-mutant (Mut)-reverse (R) and EGE-WYS-006-A-WT-R sequences were mixed into the same tube for genotype identification. WT-F---Mut-R refers to the bands amplified by primers WT-F

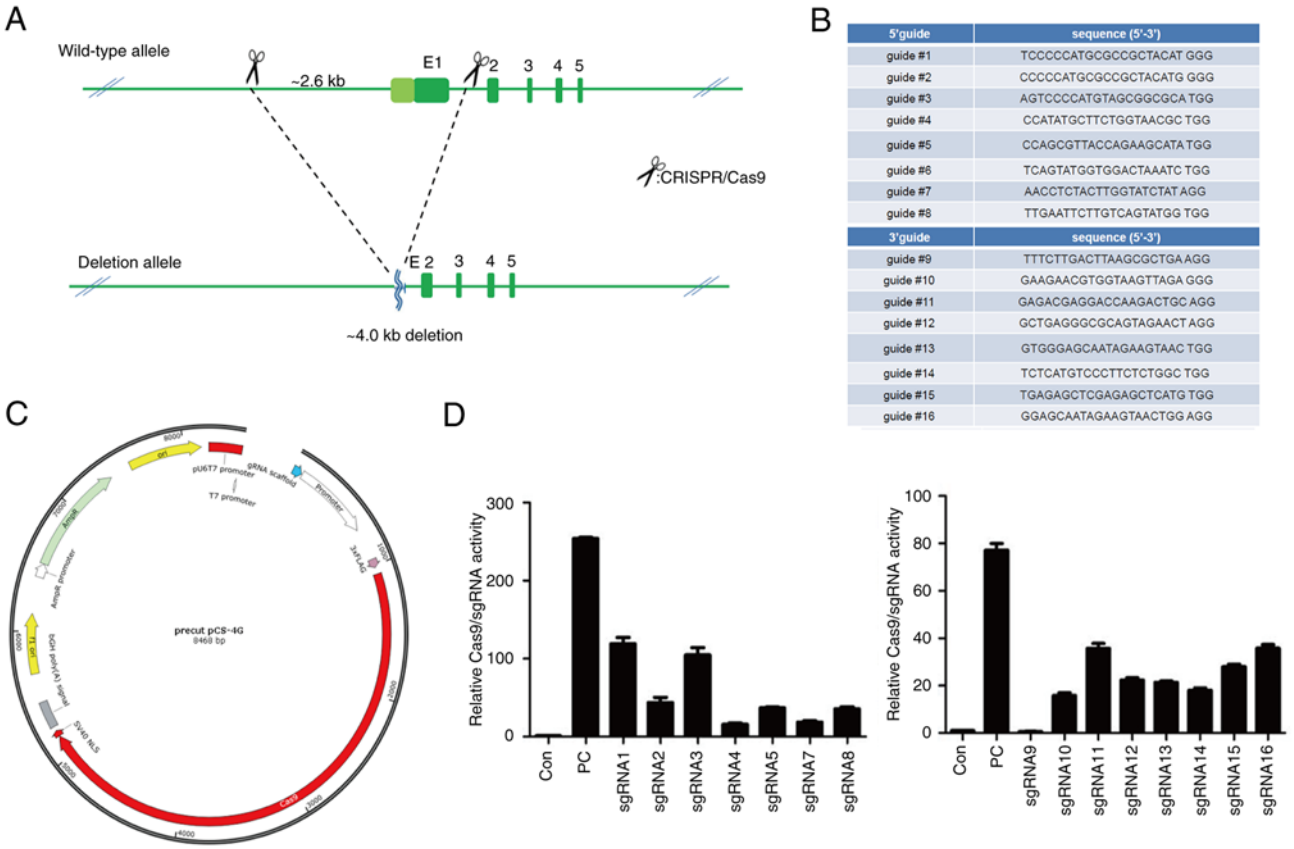

Figure 1. Npr1 gene knockout and physiological indexes. (A) Npr1 gene knockout strategy. (B) sgRNAs and corresponding target sequences. (C) pCS-4G carrier map. (D) Detection of Cas9/sgRNA activity. Npr1, natriuretic peptide receptor 1; sgRNA, single guide RNA; Con, control; CRISPR, clustered Regularly Interspaced Short Palindromic Repeats.

and Mut-R. WT-F---WT-R refer to bands amplified by primers WT-F and WT-R (Fig. S1). The following primer pairs were used for PCR: EGE-WYS-006-A-WT-F, 5'-CCCAAACT CCAGCGTTACCAGAAGC-3' and EGE-WYS-006-A-WT-R, 5'-CCTGAGATATTGAAAAGCTAGCCAC-3' and EGE-WYS-006-A-Mut-R, 5'-GACGAGGACCAAGACTGC AGGAAG-3'. The reaction system consisted of a total of 15 μl of mixed solution, including EGE-WYS-006-A-WT-F, EGE-WYS-006-A-WT-R and EGE-WYS-006-A-Mut-R 0.8 μl respectively, dd H_2O 12.1 μl, 5xGreen GoTaq buffer (M3005, Promega) 4 μl and amplification template 1 μl. The following conditions were used for PCR: Initial denaturation at 95 ˚C for 15 sec, annealing at 62 ˚C for 20 sec and extension at 72˚C for 30 sec for 30 cycles. Electrophoresis was performed using 1% agarose under conditions of 90 V for 30 min and visualized through gel imaging system (Image Quant LAS 4000, General Electric Company). For WT mice, there were theoretically two types of WT-F-Mut-R and WT-F-WT-R band; however, only WT-F-WT-R band was selected, with a size of 466 bp because the WT-F-Mut-R band exceeded the length of WT-F-WT-R and PCR products did not reach the expected length. For heterozygous mice, there were WT-F-WT-R and WT-F-Mut-R bands with sizes of 466 and 357 bp, respectively.

Western blotting. Western blotting analysis was conducted as previously described (20). Briefly, the tissue was harvested with a surgical blade and lysed with RIPA lysis buffer (cat. no. R0010; Beijing Solarbio) for 30 min at 4˚C. The samples were quantified by BCA) kit (cat. no. P0009; Beyotime Biotechnology) and heated in boiling water for 5 min and 30 ug total protein/lane was loaded and separated using SDS-PAGE on 10% gel and transferred onto PVDF membranes (cat. no. IEVH07850, Millipore). Membranes were blocked for 2 h with 5% milk at room temperature. Subsequently, membranes were incubated with the following primary antibodies: Anti-NPR1 (cat. no. ab14356; Abcam, 1:1,000); anti-SGK1 (cat. no. DF6188; Affinity Biosciences, Ltd.; 1:1000) and anti-β-actin (cat. no. 81115-1-RR, Proteintech, 1:10,000) overnight at 4˚C. Following primary incubation, membranes were incubated with Goat Anti-Rabbit IgG H&L (horseradish peroxidase) secondary antibody (cat. no. ab205718; Abcam, 1:1,000) for 1.5 h at room temperature. Bands were visualized using ultra-sensitive ECL chemiluminescence kit (P0018AS, Beyotime Institute of Biotechnology) by chemiluminescence imaging system (ChemiDoc XRS, Bio-Rad). Data were analyzed using Image J (version 1.8.0, National Institutes of Health).

IHC analysis. The relative levels of the target proteins were visualized via IHC using primary antibodies against NPR1 (cat. no. ab14356; Abcam, 1:1000) and SGK1 (cat. no. ET1610-19; HUABIO, 1:1000) as previously described (21). The stained tissue was observed in four randomly selected fields of view using a light microscope (DM6B, Leica) to compare expression levels of these proteins. The magnification was x200.

IF analysis. IF analysis was performed as previously described (22). The heart tissues were frozen at -20˚C and cut into 5-μm-thick sections with freezing microtome to incubate with primary antibodies against NPR1 (cat. no. sc-137041, Santa Cruz Biotechnology, Inc.; 1:1000) and SGK1 (cat. no. ET1610-19; HUABIO, 1:1,000), and then reacted with secondary antibodies Goat anti-Rabbit IgG (H+L) Secondary Antibody, DyLight™ 488 (cat. no. S6002, ReportBio,1:10000) and Mouse IgG (H&L) Dylight 549 conjugated (cat. no. S1411, ReportBio, 1:10,000). The stained tissue was observed in four randomly selected fields of view by fluorescence microscope (DM6 B, Leica) and compared expression levels of these proteins by Image J (version 1.8.0, National Institutes of Health). The magnification was x400 and x100.

Blood pressure measurement. Blood pressure was measured using the tail-cuff method by an individual blinded to the genotype (23). After 5 days of training, the blood pressure of each animal was measured as the mean of ≥4 sessions on each of 5 days.

Transthoracic echocardiography. Mice were anesthetized via inhalation of 1-4% isoflurane, the chest was depilated and echocardiograms were obtained using an echocardiograph (HP Sonos 2500 Ultrasound System; Hewlett-Packard, Inc.). A transducer (7.5 MHz) was utilized to obtain two-dimensional guided M-type trajectories of the left ventricular short axis cross-section at the papillary apex, as previously described (24).

Statistical analysis. All experiments were repeated at least four times. Data are presented as the mean ± standard error of the mean. The data were compared using unpaired t test or one-way ANOVA followed by Tukey's post hoc test. Statistical analysis was performed using SPSS 21.0 (IBM Corp). $P<0.05$ was considered to indicate a statistically significant difference.

Results

Construction of the Npr1$^{+/-}$ mouse model. The structure of the Npr1 gene was showed in National Center for Biotechnology Information (NCBI) (https://www.ncbi.nlm.nih.gov/gene/?term=18160) and exon 1 (including the 5'-UTR) was deleted. The two sgRNAs were designed to be located at 2.6 kb upstream of ATG and downstream of exon 1, resulting in a 4.0-kb genome deletion, which was the goal of Npr1 knockout process (Fig. 1A). The mouse model was prepared using an EGE system based on CRISPR/Cas9. A total of eight sgRNA sequences were designed and synthesized into oligos that were ligated into the pCS-4G vector using the Gibson method (Fig. 1B and C). Two sgRNAs, EGE-WYS-006-A-sgRNA 1 and EGE-WYS-006-A-sgRNA 12, were screened using the CRISPR/Cas9 activity detection method (Fig. 1D).

Changes to physiological indexes after the successful construction of the Npr1$^{+/-}$ mouse model. In western blotting, lanes 1 and 2 had one band, representing the WT mice (n=2). Lanes 3, 4, 5, 6 and 7 had two bands (n=5), which were specific for the heterozygous mice. The two types of bands represented WT (n=4) and the heterozygous mice (n=7), respectively. There was no band in lane 8, which represented the negative control (Fig. 2A). The protein levels of NPR1 in the heart and renal tissue of Npr1$^{+/-}$ mice decreased significantly compared with those in WT mice, as demonstrated through western blotting, IF and IHC assay (Fig. 2B-F). Compared with those in the WT group, the weight, heart rate and blood pressure of Npr1$^{+/-}$ mice increased significantly, indicating that Npr1 heterozygosity caused changes in the physiological indices (Fig. 2G-I).

Glucocorticoids reverse cardiac dysfunction associated with Npr1 gene knockdown. Cardiac function deteriorated in Npr1$^{+/-}$ mice; left ventricular ejection fraction (EF%) and left ventricular shortening fraction (FS%) in Npr1$^{+/-}$ mice decreased significantly, while left ventricular systolic and diastolic diameter increased in the Npr1$^{+/-}$ mice compared with those in WT mice. Dexamethasone improved cardiac function and parameters in the Npr1$^{+/-}$ mice (Fig. 3A-G). A characteristic increase in left ventricular diameter and volume was observed in the systolic and diastolic period after the Npr1 gene knockdown. However, these changes were suppressed by dexamethasone treatment (Fig. 3A-G). The heart size was also consistent with this trend (Fig. 3J). There was no significant difference between the stroke volume and cardiac output of Npr1$^{+/-}$ and WT mice (Fig. 3H-I), suggesting that heart failure observed in Npr1$^{+/-}$ mice was still at the compensatory stage.

Glucocorticoids suppress renal dysfunction in Npr1$^{+/-}$ mice. The cumulative excretion of urinary sodium, potassium, nitrogen and creatinine in 12 h in Npr1$^{+/-}$ mice decreased significantly compared with that in the WT mice. Dexamethasone abolished the effects of Npr1 knockdown on renal function (Fig. 4B, C, E and G).

The increase in serum creatinine and the decrease in creatinine clearance and urea nitrogen excretion in Npr1$^{+/-}$ mice reflected impaired renal excretory function; dexamethasone reversed the impaired renal excretory function in these mice (Fig. 4D, F and G). Urine volume of the Npr1$^{+/-}$ group did not change significantly; however, dexamethasone significantly increased urine volume compared with that in the WT group (Fig. 4A).

Glucocorticoids inhibit SGK1 expression and upregulate NPR1 in Npr1$^{+/-}$ mice. In the renal tissues of mice, upregulation of SGK1 expression was observed in the Npr1$^{+/-}$ group compared with that in the WT group (Fig. 5A-C). However, dexamethasone treatment decreased SGK1 expression and increased NPR1 expression in Npr1$^{+/-}$ mice (Fig. 5A-C).

SGK1 inhibitor GSK650394 improves cardiorenal function in Npr1$^{+/-}$ mice. To explore the association between the improvement of cardiorenal function caused by dexamethasone and downregulation of SGK1 expression, SGK1 inhibitor GSK650394 was used to inhibit expression of SGK1 and to observe whether the cardiorenal function of Npr1$^{+/-}$ mice was improved. IHC analysis demonstrated that SGK1 inhibitor GSK650394 significantly inhibited expression of SGK1 (Fig. 6A). Compared with those in the Npr1$^{+/-}$ mice, FS%, EF% and left ventricular diastolic diameter and volume in the Npr1$^{+/-}$ + GSK650394 group decreased significantly, reflecting an improvement in cardiac function (Fig. 6B-F). Furthermore, urinary sodium and potassium excretion and

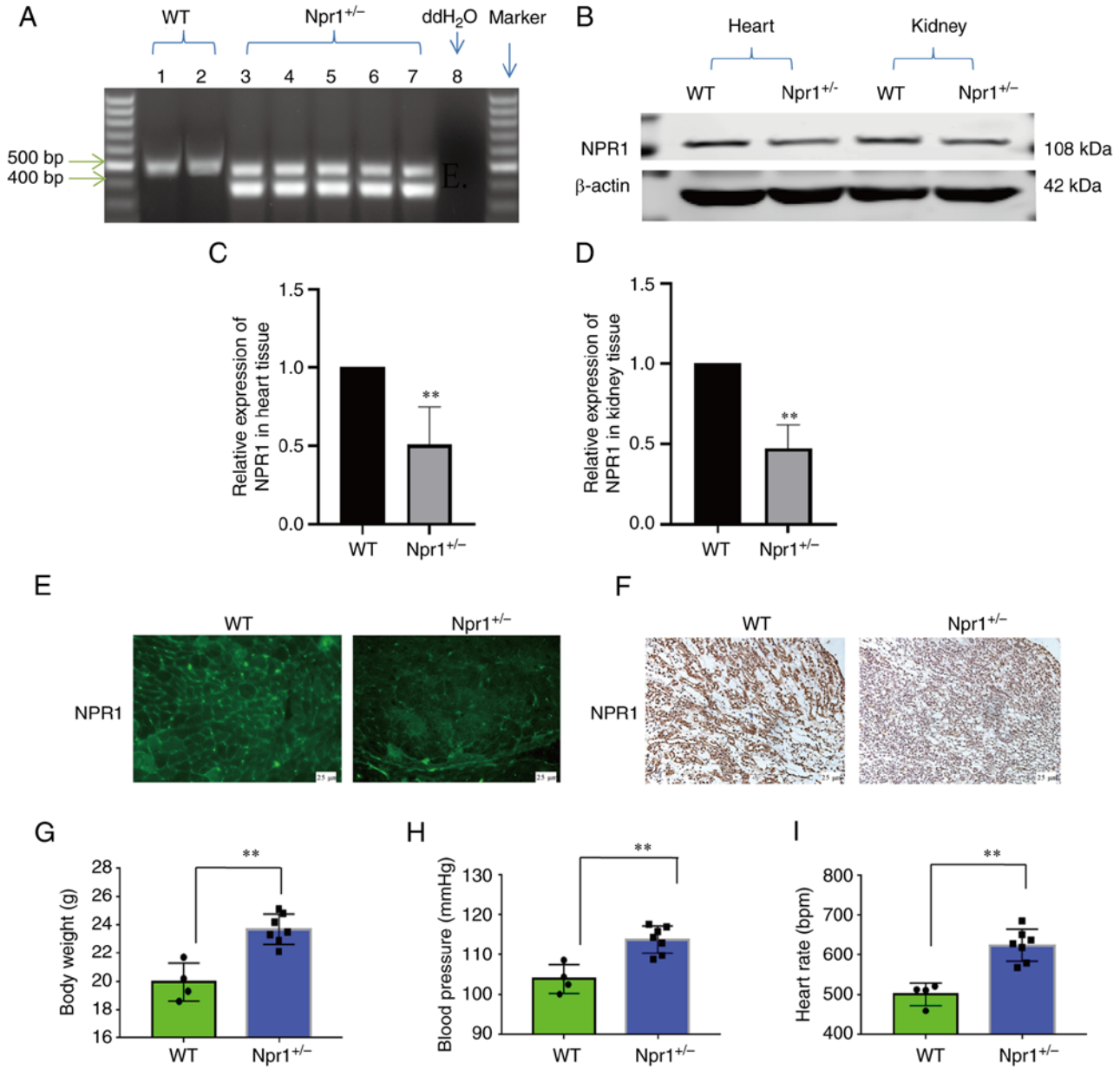

Figure 2. Physiological indexes. (A) Genotype identification-specific PCR and agarose gel electrophoresis. Lanes 1 and 2 had one band, representing results for two of the four WT mice. Lanes 3-7 had two band, representing results for four of the seven heterozygous mice. (B) NPR1 expression levels in heart and renal tissue of Npr1$^{+/-}$ and WT mice using western blotting. (C) Analysis of NPR1 expression levels in heart tissue of Npr1$^{+/-}$ and WT mice. (D) Analysis of NPR1 expression levels in kidney tissue of Npr1$^{+/-}$ and WT mice. (E) NPR1 expression levels in the heart tissues of Npr1$^{+/-}$ and WT mice using immunofluorescence (magnification, x400; scale bar, 25 μm). (F) NPR1 expression levels in kidney tissues of Npr1$^{+/-}$ mice and WT mice using immunohistochemistry (magnification, x200; scale bar, 50 μm). (G) Body weight, (H) blood pressure of Npr1$^{+/-}$ and WT mice. (I) heart rate of Npr1$^{+/-}$ and WT mice. **P<0.01 vs. WT. Npr1, natriuretic peptide receptor 1; WT, wild-type.

creatinine clearance rate of the kidney increased in the Npr1$^{+/-}$+GSK650394 group, indicating renal function improvement (Fig. 6G-I).

Discussion

Cardiorenal syndrome is a complex pathophysiological disorder of the heart and kidney in which acute or chronic dysfunction in one organ may induce acute or chronic dysfunction in the other (25,26). Cardiorenal syndrome models induced by operation (such as nephrectomy and renal ischemia/reperfusion), combined operation (such as partial nephrectomy combined with coronary artery ligation), drugs and other factors have been reported (25,27-29). However, the aforementioned animal models of cardiorenal syndrome are associated with low modelling success rate, high mortality and asynchronous damage to the heart and kidney. Therefore, the establishment of a stable, reliable and effective animal model of cardiorenal syndrome is needed to study the pathogenesis and treatment of this condition.

Previous studies found that the knockout of NPR1 decreases cardiac contractility and promotes cardiac remodelling (30,31). Moreover, the downregulation of NPR1 in the kidneys is a key cause of natriuretic peptide resistance (20,32,33).

The present study established a novel model of cardiorenal syndrome and discussed the potential mechanisms underlying

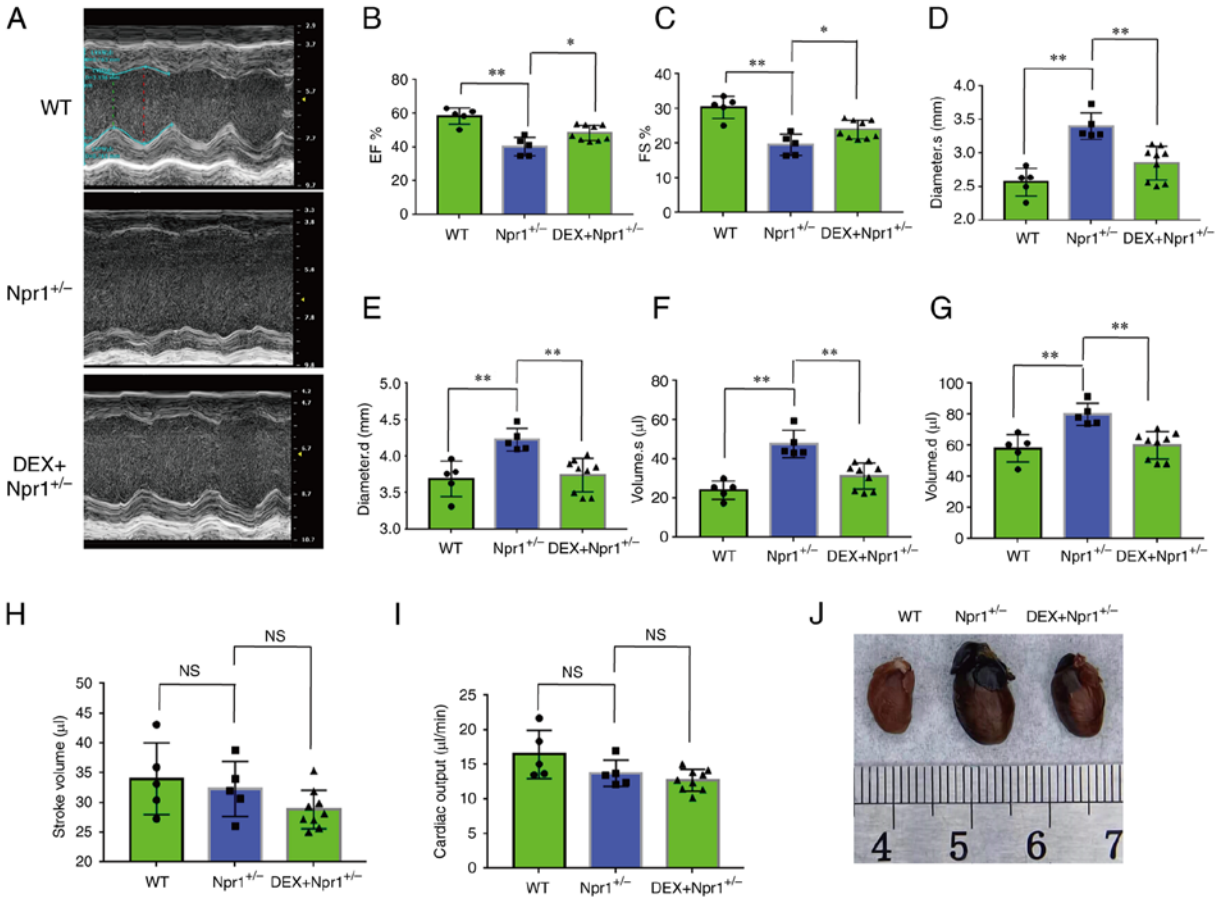

Figure 3. Echocardiography analysis. (A) Echocardiography analysis of WT (n=5), Npr1$^{+/-}$ (n=5) and DEX + NPR (n=9) mice. (B) EF%. (C) Analysis of FS% (D) Analysis of diameter.s. (E) Diameter.d. (F) Analysis of volume.s. (G) Analysis of volume.d. (H) Analysis of stroke volume. (I) Cardiac output. (J) Heart size of WT, Npr1$^{+/-}$ and DEX + Npr1$^{+/-}$ mice *P<0.05, **P<0.01. NS, not significant; Npr1, natriuretic peptide receptor 1; WT, wild-type; EF, ejection fraction; FS, fractional shortening; s, systolic; d, diastolic; DEX, dexamethasone.

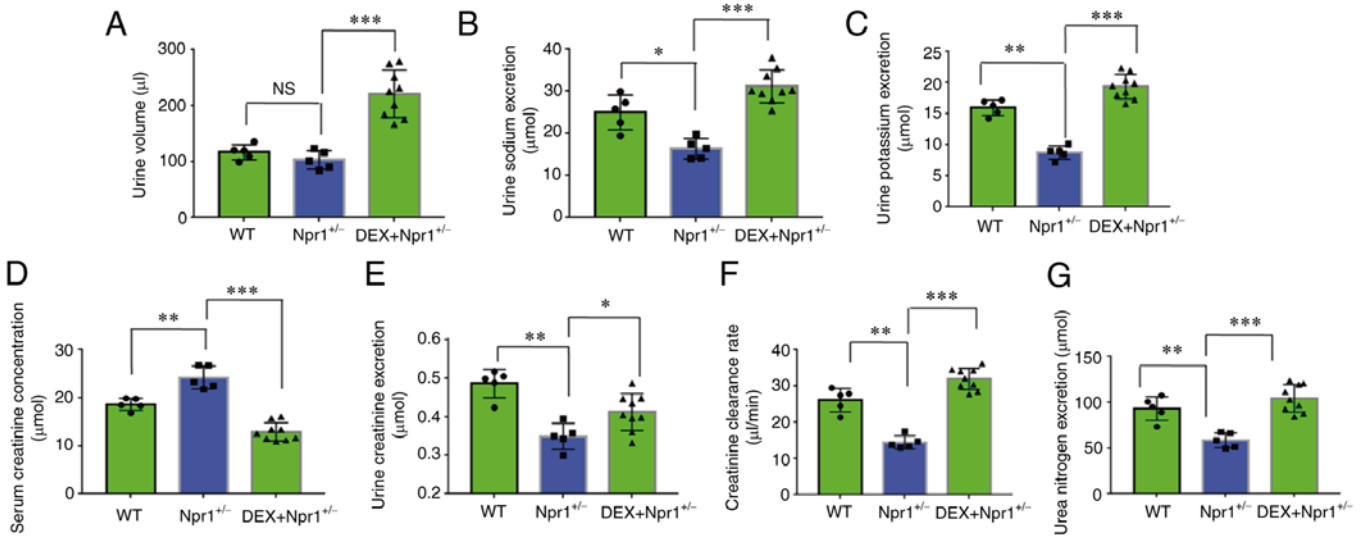

Figure 4. Physiological indexes of renal function. (A) Urinary volume (B) Analysis of urinary sodium. (C) Urinary potassium. (D) Analysis of urinary serum. (E) Analysis of urinary creatinine. (F) Creatinine clearance rate. (G) Analysis of urea nitrogen. WT (n=5), Npr1$^{+/-}$ (n=5) and DEX + Npr1$^{+/-}$ mice (n=9). *P<0.05, **P<0.01 and ***P<0.001. NS, not significant; Npr1, natriuretic peptide receptor 1; WT, wild-type; DEX, dexamethasone.

regulation of cardiac and renal functions by glucocorticoids (dexamethasone). Npr1$^{+/-}$ mice showed an increase in body weight, heart rate and blood pressure but a decrease in left ventricular EF% and FS%, compared with WT mice. The ventricular dilation and left ventricular volume also increased in these Npr1$^{+/-}$ mice and these effects were suppressed by

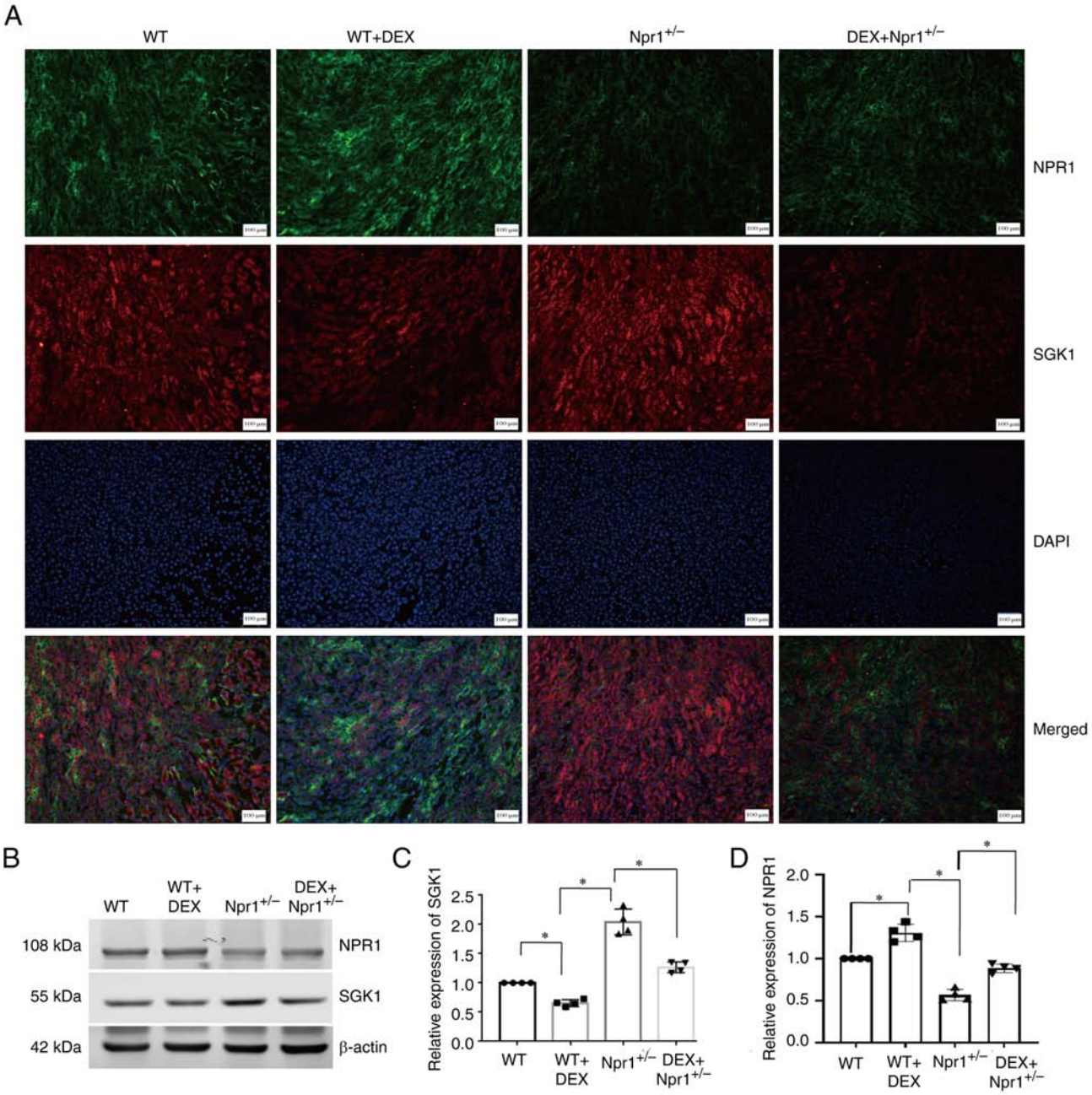

Figure 5. NPR1 and SGK1 expression levels. (A) Analysis of NPR1 and SGK1 expression levels in the heart tissue of WT, Npr1$^{+/-}$, WT + DEX and Npr1$^{+/-}$ + DEX mice (n=4/group) using immunofluorescence (magnification, x100; scale bar, 100 μm). (B) Analysis of NPR1 and SGK1 expression levels in the heart tissues of WT, Npr1$^{+/-}$, WT + DEX and DEX + Npr1$^{+/-}$ mice using western blotting. (C) Relative expression of SGK1 using western blotting. (D) Relative expression levels of NPR1 using western blotting. *P<0.05. Npr1, natriuretic peptide receptor 1; WT, wild-type; DEX, dexamethasone; SGK1, serum/dexamethasone regulated kinase 1.

dexamethasone (a kind of glucocorticoids) treatment for 12 h. Sodium and potassium excretion capacity and creatinine clearance rate of Npr1$^{+/-}$ mice decreased significantly, but dexamethasone reversed the renal function damage caused by Npr1 knockdown. Npr1 gene knockdown did not have a significant effect on stroke volume and cardiac output, which indicated that cardiac function of Npr1$^{+/-}$ mice may be in a compensatory period to maintain survival of Npr1 $^{+/-}$ mice, although the cardiac function decreased significantly.

Previous studies have showed that targeted knockout of ANP or NPR1 can lead to severe chronic arterial hypertension (34,35). However, other reports have showed that cardiac Npr1 gene-specific or systemic knockout has no impact on the ventricular EF% in mice (10,32). This is different from the present results and may be because, despite the same gene knockout protocol being selected, the cutting sites may be slightly different (after sgRNA-mediated cutting) (36). Further experiments are needed to verify these discrepancies.

Previous studies have showed that a lack of SGK1 could protect against high-salt diet-induced hypertension and prevent development of hypoxia-induced pulmonary arterial hypertension (37,38), while upregulation of SGK1 in the kidneys could upregulate ENaC expression, promoting sodium reabsorption and decreasing renal sodium excretion (14,15).

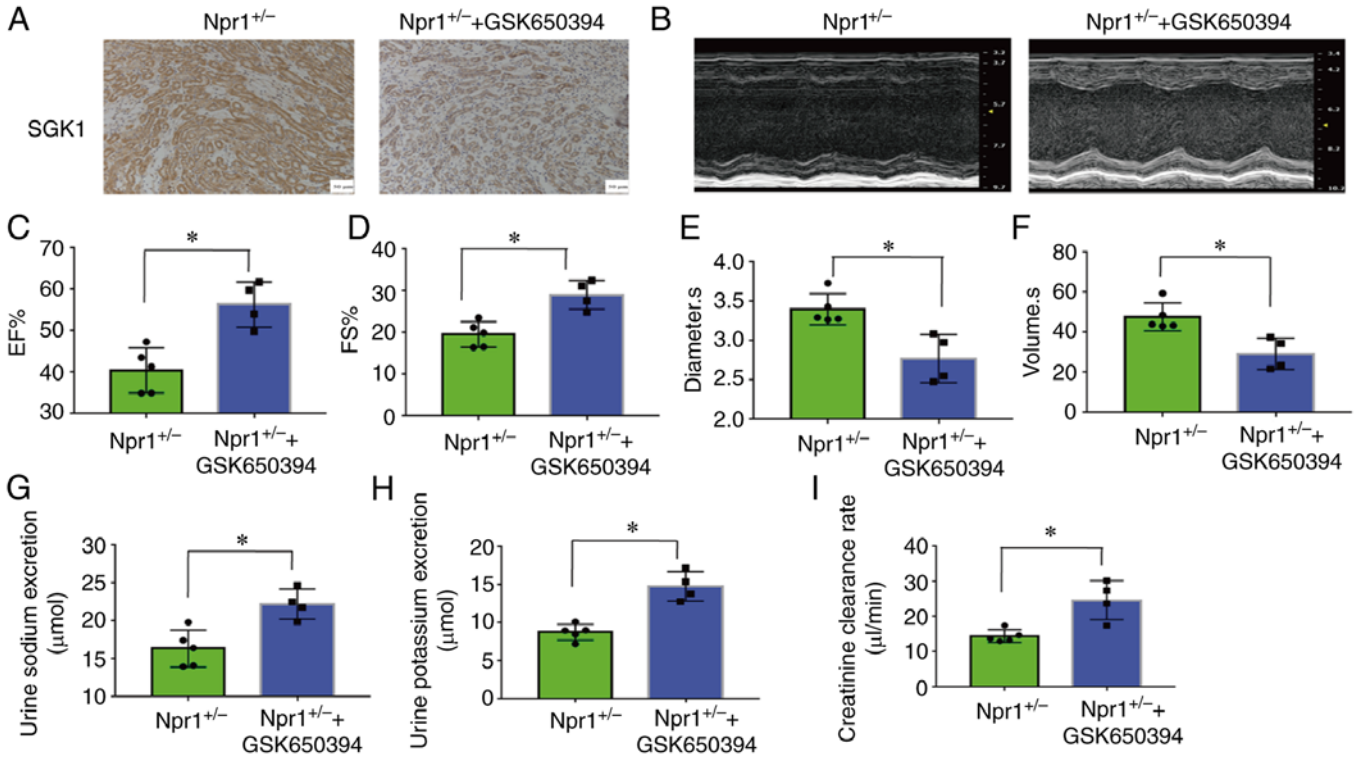

Figure 6. Effect of GSK650394 on cardiac and renal function. (A) Analysis of SGK1 expression levels in renal tissue of Npr1$^{+/-}$ (n=6) and Npr1$^{+/-}$ + GSK650394 (n=4) mice using immunohistochemistry (magnification, x200; scale bar, 50 μm). (B) Echocardiography. (C) Analysis of EF%. (D) Analysis of FS%. (E) Analysis of diameter.s. (F) Analysis of volume.s. (G) Analysis of urinary sodium. (H) Analysis of potassium excretion. (I) Analysis of creatinine clearance. *P<0.05. WT, wild-type; Npr1, natriuretic peptide receptor 1; EF, ejection fraction; FS, fractional shortening; s, systolic.

In addition, our previous studies showed that glucocorticoids promote expression of NPR1, decrease the expression of SGK1 and improve the pathological state of water and sodium retention in mice with heart failure (20,39). However, the association between NPR1 and SGK1 remains unclear. In the present study, following dexamethasone treatment, SGK1 was significantly downregulated; this trend was significantly inhibited by knocking down NPR1, which illustrated that dexamethasone negatively regulated SGK1 expression by promoting NPR1 upregulation. After GSK650394 specifically inhibited expression of SGK1, cardiac and renal function improved significantly, which indicated that the SGK1 downregulation caused by dexamethasone was associated with improved cardiac and renal function. Although previous studies have showed that glucocorticoids mainly upregulated the expression of SGK1 in isolated cells (40,41), SGK1 expression in the renal medulla decreased significantly 12 h after dexamethasone administration. This may be because the levels of aldosterone (a kind of mineralocorticoid) are higher in kidney tissues than that in isolated cells *in vivo*. Aldosterone first binds to the mineralocorticoid receptor (MR), preventing the activation of the Glucocorticoids/MR pathway and mineralocorticoid activity caused by the interactions between glucocorticoids and MR. In isolated cells, because of the lack of aldosterone, glucocorticoids activate MR, resulting in mineralocorticoid activity, which promotes expression of SGK1 (42). Further experiments are needed to verify the aforementioned hypothesis and elucidate the specific mechanisms underlying these phenomena. The current study provided evidence to support the clinical application of glucocorticoids to alleviate cardiorenal syndrome. However, there were several limitations. First, the present study was performed in the Npr1$^{+/-}$ mouse model and further research is needed in Npr1 gene knockout mice. Second, the experiment focused on animals; cytological studies are needed to uphold the present findings. Third, weighting mouse hearts and hematoxylin-eosin or Masson staining were not performed; pathological phenotypical changes of the heart should be investigated in follow-up experiments.

In the present study, a novel cardiorenal syndrome was constructed in Npr1$^{+/-}$ mice. Dexamethasone) ameliorated cardiorenal dysfunction in these mice by activating the NPR1/SGK1 pathway. These findings provided a novel model for study of cardiorenal syndrome and insight into the treatment of cardiorenal diseases. Thus, dexamethasone) may serve as a potential therapeutic candidate and the NPR1/SGK1 pathway may serve as a therapeutic target for treatment of cardiorenal syndrome.

Acknowledgements

Not applicable.

Funding

The present study was supported by The National Natural Science Foundation of China (grant no. 81670357).

Availability of data and materials

The datasets used and/or analyzed during the current study are available from the corresponding author on reasonable request.

Authors' contributions

YMH wrote the manuscript and conducted experiments. TXL conducted this experiment. SYL and XRZ collected data and the literature. YL, DYL, WML and KSL collected and interpreted the data, and drew the figures. LQY raised mice and acquired the data. CL designed the study, conducted data analysis, and revised the manuscript. YMH and TXL confirm the authenticity of all the raw data. All authors have read and approved the final manuscript.

Ethics approval and consent to participate

All research involving animals was reviewed and approved by the Ethics Review Committee for Animal Experimentation of the Hebei Medical University, Shijiazhuang, China (approval no. 20210909).

Patient consent for publication

Not applicable.

Competing interests

The authors declare that they have no competing interests.

References

1. Forte M, Madonna M, Schiavon S, Valenti V, Versaci F, Zoccai BG, Frati G and Sciarretta S. Cardiovascular pleiotropic effects of natriuretic peptides. Int J Mol 20: 3874-3892, 2019.
2. Nakagawa Y, Nishikimi T and Kuwahara K: Atrial and brain natriuretic peptides: Hormones secreted from the heart. Peptides 111: 18-25, 2019.
3. Yu Y, Chen Y, Mei C, Li N, Wu K and Huang D: C-type natriuretic peptide stimulates function of the murine Sertoli cells via activation of the NPR-B/cGMP/PKG signaling pathway. Acta Biochim Pol 68: 603-609, 2021.
4. Vinnakota S and Chen HH: The importance of natriuretic peptides in cardiometabolic diseases. J Endocr Soc 4: bvaa052, 2020.
5. Jansen HJ, Mackasey M, Moghtadaei M, Liu Y, Kaur J, Egom EE, Tuomi JM, Rafferty SA, Kirkby AW and Rose RA: NPR-C (natriuretic peptide receptor-C) modulates the progression of angiotensin II-mediated atrial fibrillation and atrial remodeling in mice. Circ Arrhythm Electrophysiol 12: e006863, 2019.
6. López-Morales MA, María CR, Burguete MC, Jover-Mengual T, Aliena-Valero A, Centeno JM, Alborch E, Salom JB, Torregrosa G and Miranda FJ: Molecular mechanisms underlying the neuroprotective role of atrial natriuretic peptide in experimental acute ischemic stroke. Mol Cell Endocrinol 472: 1-9, 2018.
7. Sun F, Zhou K, Tian KY, Wang J, Qiu JH and Zha DJ: Atrial natriuretic peptide improves neurite outgrowth from spiral ganglion neurons in vitro through a cGMP-dependent manner. Neural Plasticity 28: 8831735, 2020.
8. Joubert S, Jossart C, McNicoll N and De Léan A: Atrial natriuretic peptide-dependent photolabeling of a regulatory ATP-binding site on the natriuretic peptide receptor-A. FEBS J 272: 5572-5583, 2010.
9. Podewin T, Broichhagen J, Frost C, Groneberg D, Ast J, Meyer-Berg H, Nicholas HF, Friebe A, Zacharias M, Hodson DJ, *et al*: Optical control of a receptor-linked guanylyl cyclase using a photoswitchable peptidic hormone. Chem Sci 8: 4644-4653, 2017.
10. Kilic A, Velic A, De Windt LJ, Fabritz L, Voss M, Mitko D, Zwiener M, Baba HA, van Eickels M, Schlatter E and Kuhn M: Enhanced activity of the myocardial Na+/H+ exchanger NHE-1 contributes to cardiac remodeling in atrial natriuretic peptide receptor-deficient mice. Circulation 112: 2307-2317, 2005.
11. Oliver PM, Fox JE, Kim R, Rockman HA, Kim HS, Reddick RL, Pandey KN, Milgram SL, Smithies O and Maeda N: Hypertension, cardiac hypertrophy, and sudden death in mice lacking natriuretic peptide receptor A. Proc Natl Acad Sci USA 94: 14730-14735, 1997.
12. Prerna K, Krishna P and Kailash P: SAT-046 modulation of histone 3 acetylation and methylation enhances the expression and function of Nprl in haplotype mice. J Endocr Soc 3 (Suppl 1): SAT-046, 2019.
13. Long C, Liu H, Zhan W, Chen L, Wu A, Yang L and Chen S: Null function of Nprl disturbs immune response in colonic inflammation during early postnatal stage. Inflammation 45: 2419-2432, 2022.
14. Xiu F, Yu ZQ, Yang BW, Li M, Xian XM, Meng Z, Guo LR and Wang S: Aldosterone alleviates lipopolysaccharide-induced acute lung injury by regulating epithelial sodium channel through PI3K/Akt/SGK1 signaling pathway. Mol Cell Probes 57: 101709, 2021.
15. Chen M, Chen Q, Li Y, Yang Z, Taylor EW and Zhao LJ: A G-quadruplex nanoswitch in the SGK1 promoter regulates isoform expression by K^+/Na^+ balance and resveratrol binding. Biochim Biophys Acta Gen Subj 1865: 129778-129797, 2021.
16. Chen S, McCormick JA, Prabaker K, Wang J, Pearce D and Gardner DG: Sgk1 mediates osmotic induction of NPR1 gene in rat inner medullary collecting duct cells. Hypertension 43: 866-871, 2004.
17. Holtwick R, Gotthardt M, Skryabin B, Steinmetz M, Potthast R, Zetsche B, Hammer RE, Herz J and Kuhn M: Smooth muscle-selective deletion of guanylyl cyclase-A prevents the acute but not chronic effects of ANP on blood pressure. Proc Natl Acad Sci USA 99: 7142-7147, 2002.
18. Shola DTN, Yang C, Kewaldar VS, Kar P and Bustos V: New additions to the CRISPR toolbox: CRISPR- CLONInG and CRISPR-CLIP for donor construction in genome editing. CRISPR J 3: 109-122, 2020.
19. Chan W, Chandra S, David P and Samuel K: A comparison and optimization of methods and factors affecting the transformation of Escherichia coli. Biosci Rep 33: e00086, 2020.
20. Zhu X, Huang Y, Li S, Ge N, Li T, Wang Y, Liu KS and Liu C: Glucocorticoids reverse diluted hyponatremia through inhibiting arginine vasopressin pathway in heart failure rats. J Am Heart Assoc 9: e014950, 2020.
21. Magaki S, Hojat SA, Wei B, So A and Yong WH: An introduction to the performance of immunohistochemistry. Methods Mol Biol 1897: 289-298, 2019.
22. Odell ID and Cook D: Immunofluorescence techniques. J Invest Dermatol 133: 1-4, 2013.
23. Feng R, Ullah M, Chen K, Ali Q, Lin Y and Sun Z: Stem cell-derived extracellular vesicles mitigate ageing-associated arterial stiffness and hypertension. J Extracell Vesicles 9: 1783869, 2020.
24. Zhou X, Li Z, Qi M, Zhao P, Duan Y, Yang G and Yan LJ: Brown adipose tissue-derived exosomes mitigate the metabolic syndrome in high fat diet mice. Theranostics 10: 8197-8210, 2020.
25. Ronco C, Bellasi A and Lullo LD: Cardiorenal syndrome: An overview. Adv Chronic Kidney Dis 25: 382-390, 2018.
26. Kumar U, Wettersten N and Garimella PS: Cardiorenal syndrome. Cardiol Clin 37: 251-265, 2019.
27. Liu S, Kompa AR, Kumfu S, Nishijima F, Kelly DJ, Krum H, Krum H and Wang BH: Subtotal nephrectomy accelerates pathological cardiac remodelling post-myocardial infarction: Implications for cardiorenal syndrome. Int J Cardiol 168: 1866-1880, 2013.
28. Savira F, Wang BH, Edgley AJ, Jucker BM, Willette RN, Krum H, Kelly DJ and Kompa AR: Inhibition of apoptosis signal-regulating kinase 1 ameliorates left ventricular dysfunction by reducing hypertrophy and fibrosis in a rat model of cardiorenal syndrome. Int J Cardiol 310: 128-136, 2020.
29. Yang CC, Chen YT, Chen CH, Li YC, Shao PL, Huang TH, Chen YL, Sun CK and Yip HK: The therapeutic impact of entresto on protecting against cardiorenal syndrome-associated renal damage in rats on high protein diet. Biomed Pharmacother 116: 108954, 2019.
30. Kuhn M, Holtwick R, Baba HA, Perriard JC, Schmitz W and Ehler E: Progressive cardiac hypertrophy and dysfunction in atrial natriuretic peptide receptor (GC-A) deficient mice. Heart 87: 368-374, 2002.
31. Kilić A, Bubikat A, Gassner B, Baba HA and Kuhn M: Local actions of atrial natriuretic peptide counteract angiotensin II stimulated cardiac remodelling. Endocrinology 148: 4162-4169, 2007.

32. Rørth R, Jhund PS, Yilmaz MB, Kristensen SL, Welsh P, Desai AS, Køber L, Prescott MF, Rouleau JL, Solomon SD, *et al*: Comparison of BNP and NT-proBNP in patients with heart failure and reduced ejection fraction. Circ Heart Failure 13: e006541, 2020.
33. Richards AM and Januzzi JL: Are some patients with acute heart failure ANP-deficient? JACC Heart Fail 7: 899-901, 2019.
34. Demerath T, Staffel J, Schreiber A, Valletta D and Schweda F: Natriuretic peptides buffer renin-dependent hypertension. Am J Physiol Renal Physiol 306: 1489-1498, 2014.
35. Li Y, Madiraju P and Anand-Srivastava MB: Knockdown of natriuretic peptide receptor-A enhances receptor C expression and signalling in vascular smooth muscle cells. Cardiovasc Res 93: 350-359, 2012.
36. Skryabin BV, Holtwick R, Fabritz L, Kruse MN, Veltrup I, Stypmann J, Kirchhof P, Sabrane K, Bubikat A, Voss M and Kuhn M: Hypervolemic hypertension in mice with systemic inactivation of the (floxed) guanylyl cyclase-A gene by alphaMHC-Cre-mediated recombination. Genesis 39: 288-298, 2010.
37. Huang DY, Boini KM, Osswald H, Friedrich B, Artunc F, Ullrich S, Rajamanickam J, Palmada M, Wulff P, Kuhl D, *et al*: Resistance of mice lacking the serum- and dexamethasone-inducible kinase SGK1 against salt-sensitive hypertension induced by a high-fat diet. Am J Physiol Renal Physiol 291: 1264-1273, 2006.
38. Xi X, Zhang J, Wang J, Chen Y, Zhang W, Zhang X, Du J and Zhu G: SGK1 mediates hypoxic pulmonary hypertension through promoting macrophage infiltration and activation. Anal Cell Pathol (Amst) 2019: 3013765, 2019.
39. Li S, Huang Y, Li T, Zhu X, Li W, Liu K and Liu C: Dexamethasone s promote Na+ excretion in the renal epithelia of heart failure rats by suppressing transporter proteins involved in acute sodium loading. J Cardiovasc Pharmacol 80: 453-463, 2022.
40. Hira S, Packialakshmi B, Tang E, Tang E and Zhou X: Dexamethasone upregulates mitochondrial Tom20., Tom70., and MnSOD through SGK1 in the kidney cells. J Physiol Biochem 77: 1-11, 2020.
41. Wang HL, Yang CH, Lee HH, Kuo JC, Hur SS, Chien S, Lee OK, Hung SC and Chang ZF: Dexamethasone-induced cellular tension requires a SGK1-stimulated Sec5-GEF-H1 interaction. J Cell Sci 128: 3757-3768, 2015.
42. Robert WH, Jessica RI and Matthew AB: Dexamethasone s and renal Na+ transport: implications for hypertension and salt sensitivity. J Physiol 592: 1731-1744, 2014.